Spatially resolved thermal conductivity measurements using a thermoreflectance microprobe

A.Neubrand[1], J. Dadda[2], E. Mueller[2], S. Perlt[3], T. Höche[4]

[1] Fraunhofer Institute for Mechanics of Materials IWM, Wöhlerstraße 11, 79108 Freiburg, Germany

[2] German Aerospace Center, Institute of Materials Research, Linder Höhe, 51147 Cologne, Germany

[3] Leibniz-Institute of Surface Modification, Permoserstraße 15, 04318 Leipzig, Germany

[4] Fraunhofer Institute for Mechanics of Materials IWM, Walter-Hülse-Str. 1, 06120 Halle, Germany

A transient thermoreflectance technique capable of creating maps of the out-of-plane thermal conductivity of materials with a spatial resolution of 5 µm is presented. The applied non-contact optical microprobe uses a thin reflective metal film as temperature transducer and heat reservoir. The parameters of the experimental set-up guarantee that the heat flow is one-dimensional. Thus, relatively simple mathematical relations can be used to extract the thermal conductivity from the recorded signal shape which is important for thermal conductivity maps with a high pixel count. For reference materials (soda-lime-glass and PbTe), the determined thermal conductivities were in good agreement with bulk values, indicating a typical measurement uncertainty of 10%. For low conductivity substrates, the measuring scheme is relatively insensitive to thermal interface resistance. Thermal conductivity maps of Lead-Antimony-Silver-Tellurium (LAST) surfaces showed distinct features which could be correlated with optical surface micrographs. The local conductivity fluctuations can possibly be attributed to local changes in the chemical composition and secondary phase formation.

Corresponding author:

Dr. Achim Neubrand

achim.neubrand@iwm.fraunhofer.de

Phone: +49 761 5142-282

FAX: +49 761 5142-510

Keywords: Thermal Conductivity, Thermoreflectance, LAST, Microanalysis

1. Introduction

Recently, high efficiency thermoelectric materials based on Lead-Antimony-Silver-Tellurium compounds (LAST) have attracted considerable attention. Distinct Ag and/or Sb-rich nanoscale and microscale secondary phases are commonly observed in LAST and are supposed to be responsible for the particularly low thermal conductivity κ in bulk LAST. Thus, the evaluation of κ of these phases is of considerable scientific interest, and the understanding of the correlation between phase composition and κ will aid in designing high-efficiency LAST materials and selecting appropriate processing routes. Ideally, the thermal conductivity of the different phases should be measured in-situ by a highly-localized measurement scheme. The aim of the work presented here was thus the development of a thermal conductivity microprobe capable of producing high resolution thermal conductivity maps of inhomogeneous thermoelectric materials.

There are a number of established photothermal methods which can determine local thermal properties. The mirage technique [1], the probe beam deflection technique [2] and frequency-domain thermoreflectance [3] are based on periodic heating of a small spot on the specimen surface with a modulated laser and measurement of the temperature fluctuations in the vicinity of the heated spot. Temperature measurement in the time domain can also be combined with pulsed laser heating. An example is time domain thermoreflectance (TDTR) which has already been used to produce thermal conductivity images of diffusion multiples [4] and thermal barrier coatings [5]. The spatial resolution of photothermal methods can reach a few micrometers range which makes thermal measurements on single grains possible [6]. The present paper reports thermal conductivity imaging on LAST thermoelectric materials based on a time domain thermoreflectance technique.

2. Experimental

Specimens

1 mm thick glass slides from soda-lime.glass (Menzel, Braunschweig, Germany, nominal composition SiO_2 72.20%, Na_2O 14.30%, K_2O 1.20%, CaO 6.40%, MgO 4.30%, Al_2O_3 1.20%) and high purity (99.999) PbTe ingot material (VUK, Čisté Kovy, s.r.o., Czech Republic) were used as homogenous substrates. Polycrystalline ingots of $AgPb_mSbTe_{2+m}$, where m = 18 (LAST-18) were produced by heating up evacuated and sealed quartz ampoules containing high purity (99.999%) Ag, PbTe, Te and Sb to 1100 °C within 5h and keeping the melt for 2.5h in a rocking furnace. The ampoules were then quenched in cold water and subjected to the following heat-

treatment in a furnace: the quenched ampoules were placed in a furnace, which was heated to 980 °C in 12h and maintained there for 2h. The furnace was then cooled to 850 °C in 13h and held there for 4h. This was followed by a further cooling from 850 °C to 450 °C at a rate of 10 °C/h and the furnace was held at 450 °C for 4h. Subsequently the furnace was cooled to room-temperature in 12h. Specimens were polished and coated with a thin Mo film of 400-1200 nm nominal thickness which acts as an optical absorber and heat reservoir. LAST-18 materials were coated additionally with a very thin (20 nm) interlayer of Cr in order to improve adhesion. The Cr and Mo layers were deposited via magnetron sputtering using an Ar pressure of $8*10^{-3}$ mbar. The film thickness was measured on simultaneously coated Si-wafer pieces with varnish marks. After sputtering, the varnish was removed with acetone and the produced step was scanned with a diamond tip (mechanical thickness-measurement device Talystep). The analyzed elevation profile results in a thickness value with an error of ±3%.

Experimental Set-Up

The principle of the used photothermal measurement system is outlined in Fig. 1. The specimen is mounted on a computer-controlled X-Y-Z-translation stage with 1 µm resolution. The specimen surface is heated by a pulsed Nd:YLF laser slightly focused to about 400 µm beam diameter (wavelength 1053 nm, pulse energy up to 300 µJ, pulse duration 8 ns, repetition rate 400 Hz). The subsequent decay of the surface temperature is measured based on the temperature induced reflectivity change of the Mo layer (thermoreflectance). A low-noise continuous wave HeNe laser was focused on the specimen surface to a diameter of 5 µm. The reflected beam is collected on a fast PIN diode coupled to a transimpedence amplifier (band width 1 kHz to 150 MHz) and the transient intensity change of the beam is recorded with a digital storage oscilloscope (band width 200 MHz) and stored in a personal computer.

Evaluation of the Signal

As the diameter of the pulsed heating laser beam (400 µm) is much larger than that of the HeNe probe laser beam (5µm) the heat flow can be regarded as one-dimensional and the temperature evolution at the surface of a coated specimen can be described by a simple integral equation if the following conditions are met: i) The optical skin depth must be small compared to the film thickness and ii) the thermal diffusivity and thermal effusivity of the film are much larger than those of the substrate iii) the thermal interface resistance between substrate and film must be small. In this case, at times long after the end of pulsed laser heating, the temperature inside the film is essentially uniform and the decay of the surface temperature $T(t, z = 0)$ is dominated by heat flow in the substrate and can be described by the following approximation according to Taketoshi et. al. [7]:

$$T(t, x=0) = F \frac{2}{\sqrt{\pi}\ C_f\ d} \exp\left(\frac{t}{\tau_s}\right) Erfc\left(\sqrt{\frac{t}{\tau_s}}\right) \quad (1)$$

Erfc is the complementary error function, F is the absorbed fluence in Jm^{-2}, C_f is the specific heat capacity of the film in $Jm^{-3}K^{-1}$ and d is the thickness of the metal film. The time constant τ_s is given by

$$\tau_s = \left(\frac{C_f d}{b_s}\right)^2 \quad (2)$$

Unless noted otherwise, the above model was applied to the measured signals, and the thermal effusivity of the substrate b_s was determined by fitting the measured signals with Eq.(1) using the time constant τ_s as a fitting parameter. The thermal conductivity κ_s of the substrate was then determined from the effusivity using the relation $\kappa_s = C_s\ b_s^2$ using the specific heat capacity C_s of the investigated materials. Thermal conductivity maps were constructed by scanning the specimen surface by repeatedly translating the specimen repeatedly by a small distance.

If one or several of the assumptions of the above approximation are inadequate, the signal can be evaluated using Laplace [8] or inverse Fourier transformation. In the latter case the surface temperature after heating with a laser pulse is described by [9]

$$T(t, z=0) = \int_{-\infty}^{+\infty} Q(\omega) \frac{\chi\left(1+\exp\left(-2\beta_f\ d\right)\right)+2\ \eta}{\kappa_f\ \beta_f\ \chi\left(1-\exp\left(-2\beta_f\ d\right)\right)+2\ \eta} \exp\left(i\omega t\right) d\omega \quad (3)$$

$$\chi = 1 + \kappa_s \beta_s R_{th} - \eta\,, \quad (4)$$

$$\eta = \frac{\kappa_s\ \beta_s}{\kappa_f\ \beta_f}\,, \quad (5)$$

$$\beta_f = \sqrt{\frac{i\omega}{k_f}}\,, \quad (6a)$$

$$\beta_s = \sqrt{\frac{i\omega}{k_s}}\,. \quad (6b)$$

κ_f and κ_s are the thermal conductivity, k_f and k_s the thermal diffusivity of the film and the substrate, respectively. R_{th} is the thermal interface resistance between film and substrate. $Q(\omega)$ is a complex source term

which describes the spectral area density of the energy coupled into the surface. $Q(\omega)$ was determined by discrete Fourier transformation of the recorded laser pulse.

3. Results and Discussion

Results for Homogenous Reference Materials

In order to test the reliability of the thermal conductivity values determined with the scheme described above, glass slides coated with Mo films of different thickness were investigated first. Fig. 2a shows the observed thermoreflectance signal together with the fitted signal according to equation (1). The signal was fitted between 200 ns and 1400 ns, the only free fitting parameter was the thermal conductivity of the glass substrate which was determined as 1.02 W/mK (using a heat capacity of 2.1 J/(cm³K)). This is in very good agreement with the reported thermal conductivity values for soda-lime glass, which cover the range of 0.92-1.14 W/mK [10]. As expected Eq.(1) cannot adequately predict the behavior below 50 ns when most of the deposited energy is still concentrated in the metal film and temperature gradients inside the film are large.

Eq. (3) predicted the behavior at such short times best if a thermal conductivity of the film of about 40 W/mK was used. The thermal interface resistance between Mo and glass is unknown, however thermal resistances of Mo/Si multilayers against different materials were studied recently [11], the highest reported thermal interface resistance of 6.0 Km²/ GW was found for an interface with Al. Assuming moderate thermal resistances of 10 Km²/GW made little change to the fitted curves and less than 1.2 % change to the fitted substrate conductivity. If a high thermal interface resistance beyond 20 Km²/GW is assumed, the determined substrate thermal conductivity differs more significantly, but considerable fitting errors in the first 20 ns occur. For the materials studied here, fitting randomly selected curves using Eq.(3) always showed that good fits in the first 100 ns could only be achieved with thermal interface resistances below 10 Km²/GW which have only a minor effect on the determined substrate conductivities. The effect of the thermal interface resistance was therefore neglected in the fits reported onwards. Note that the thermal diffusion length (i.e. the depth of the heated zone) corresponding to the involved time scales is less than 2 µm in most non-metals. Therefore the signal is affected by a region of about 5 µm diameter and less than 2 µm depth. This makes the creation of high resolution maps of the thermal conductivity of surfaces feasible. The low thermal diffusion lengths involved in the measurement make the method also suitable for measurements of the cross-plane thermal conductivity of thermoelectric films or superlattices of suitable thickness.

Table 1 shows thermal conductivity values determined by equation (1) and by equation (3) for soda-lime glass and PbTe coated with different Mo layers. Thermal conductivity values for glass coated with different film thicknesses are in reasonable agreement with the aforementioned literature values. For Mo films it was generally observed that the fitted thermal conductivity values are most consistent and the fitting errors are lowest for films of 600 to 800 nm thickness. The thermal conductivity value of a bulk PbTe specimen was determined as 1.87 W/mK and 2.00 W/mK using Eqs.(1) and (3), respectively. This compares favorably with the thermal conductivity of 1.98 W/mK derived from the thermal diffusivity measured by a commercial laser flash analyzer. Both measurements used a heat capacity of 1.271 J/(cm³K) as determined by a differential scanning calorimeter.

The approximation Eq. (1) yields consistently slightly lower values than Eq.(3), the fitting quality is nearly identical. It should be kept in mind that Eq.(3) is derived in the frequency domain and that discrete Fourier transformation of a non-periodic signal can introduce artifacts (which were minimized as much as possible by using suitable windows). Discrete Fourier transformation will therefore not yield an exact value for the thermal conductivity in our case. For PbTe, a precise fit using the finite element method was also carried out. It yielded a thermal conductivity that was almost exactly in between the values determined using Eqs. (1) and (3). However, FEM fitting is impractical for automated fitting of large maps with many pixels. As the fitting times using Eq.(1) were much shorter than using Eq.(3), the former was used unless noted otherwise.

Substrate	**Film**	**κ_s (Eq.3) in W/mK**	**RMS Error (Eq.3)**	**κ_s (Eq.1) in W/mK**	**RMS Error (Eq.1)**
Glass	389 nm Mo	1.00	32 x10^{-6}	0.88	29 x 10^{-6}
Glass	810 nm Mo	1.13	11 x10^{-6}	1.02	11 x 10^{-6}
Glass	1189 nm Mo	1.08	17 x10^{-6}	1.00	16 x 10^{-6}
PbTe	798 nm Mo	2.00	6 x 10^{-6}	1.87	5 x 10^{-6}

Table 1 Thermal conductivities κ_s determined for homogeneous materials with various metal coatings.

The upper part of Fig. 3 shows a small thermal conductivity map of the soda-lime-glass with a 810 nm Mo coating, Eq.(3). was used for evaluation of the signal. The average of all thermal conductivity values in this small map was 1.088 W/mK with a standard deviation of 0.024 W/mK (±2.2%). A large map of a different area of this specimen covering an area of 1 cm² determined using Eq.(1) showed average thermal conductivity of 0.99 W/mK with a standard deviation of 0.045 W/mK. As the material is homogeneous and amorphous, the conductivity should be uniform throughout the specimen surface. Differences in the determined thermal

conductivity are thus an indication for the relative uncertainty of the measurement (errors stemming from noise in the signal, precision of the evaluation routines, slightly different alignment of the lasers, inhomogeneity of film thickness etc.). The lower part of Fig 3 shows a thermal conductivity map of a PbTe surface coated with 798 nm Mo evaluated using Eq.(1). The local variations in thermal conductivity are small, the determined average κ_s for PbTe is 1,88 W/mK with a standard deviation of 0,11 W/mK. When the pump laser power was increased in order to create larger scans with good signal-to-noise-ratios, the film – specimen interface was damaged as the Mo film did not adhere strongly to PbTe. This showed in very large RMS errors (i.e. good fits of the measured signals with Eq.3 were not possible) with erratic and very large fluctuations of the "fitted" thermal conductivities.

Results for LAST-18

In order to improve film adhesion, all studied LAST specimens possessed a 20 nm thick Cr bond coat between the substrate and Mo. Using Eq.(1), the effect of the additional heat capacity introduced by the Cr film on the determined thermal conductivities is small, nevertheless it was taken into account when producing the maps shown below. The thermal conductivity map of a LAST-18 material coated with 598 nm Mo is shown in Fig 5, the corresponding surface region is marked A in Fig.4. Most surface areas have a thermal conductivity between 1.2 and 1.4 W/mK. A region on the top has a lower thermal conductivity of about 1 W/mK, and a region on the bottom reaches values as low as 0.4 W/mK. The whole mapped area shows a good fitting quality and the conductivity values could be reproduced in a partially overlapping scan. It is thus likely that these features in the scan really correspond to surface areas with low heat conduction. Fig. 6 is a 3-dimensional image of the area marked B in Fig 4. There is a valley with thermal conductivities below 0.8 W/mK and one isolated island with a conductivity exceeding 2 W/mK. The thermal conductivity in the encircled area should be regarded as undefined as the RMS fitting errors here are extremely high (as shown in Fig.7). These large errors are caused by surface irregularities – a pore and a mark "F" which was deliberately introduced by ion beam milling in order to facilitate unambiguous allocation of the scanned areas. The other parts of the map (including most of the valley) have low RMS fitting errors and should thus represent real surface effusivities. The variation in the thermal conductivity may be attributed to local changes in the chemical composition due to microsegregation and nano-/microscale secondary phase formations in this LAST-18 specimen [12]. The observed topography resembles Seebeck coefficient maps of the same material. Further work is underway to clearly identify the origin of the structural features observed in the thermal conductivity maps of this LAST-18 material.

4. Conclusion and Outlook

A time-domain thermoreflectance microprobe for mapping the thermal conductivity of surfaces with the following specifications was demonstrated: A spatial resolution of 5 µm, an acquisition time for a thermal conductivity image with 10000 pixels in about 12 h, a precision of the thermal conductivity of the measurement of 10 % under optimum conditions, and the possibility to check the reliability of each determined thermal conductivity data point by comparing the temperature evolution to theoretical models. Thermal conductivity maps of LAST-18 created with this microprobe showed considerable local fluctuations. It is planned to combine the acquired thermal conductivity maps of LAST materials with Seebeck coefficient maps and microstructural characterization for a better understanding of the observed thermal conductivity inhomogeneity.

Acknowledgement

Financial support of the NanokoCh project (reference number 03X3540) in the framework of the programme „Material technologies of tomorrow – Scientific pilot projects in materials science and nanotechnologies“ by the German Ministry of Education and Research (BMBF) is gratefully acknowledged.

Figures

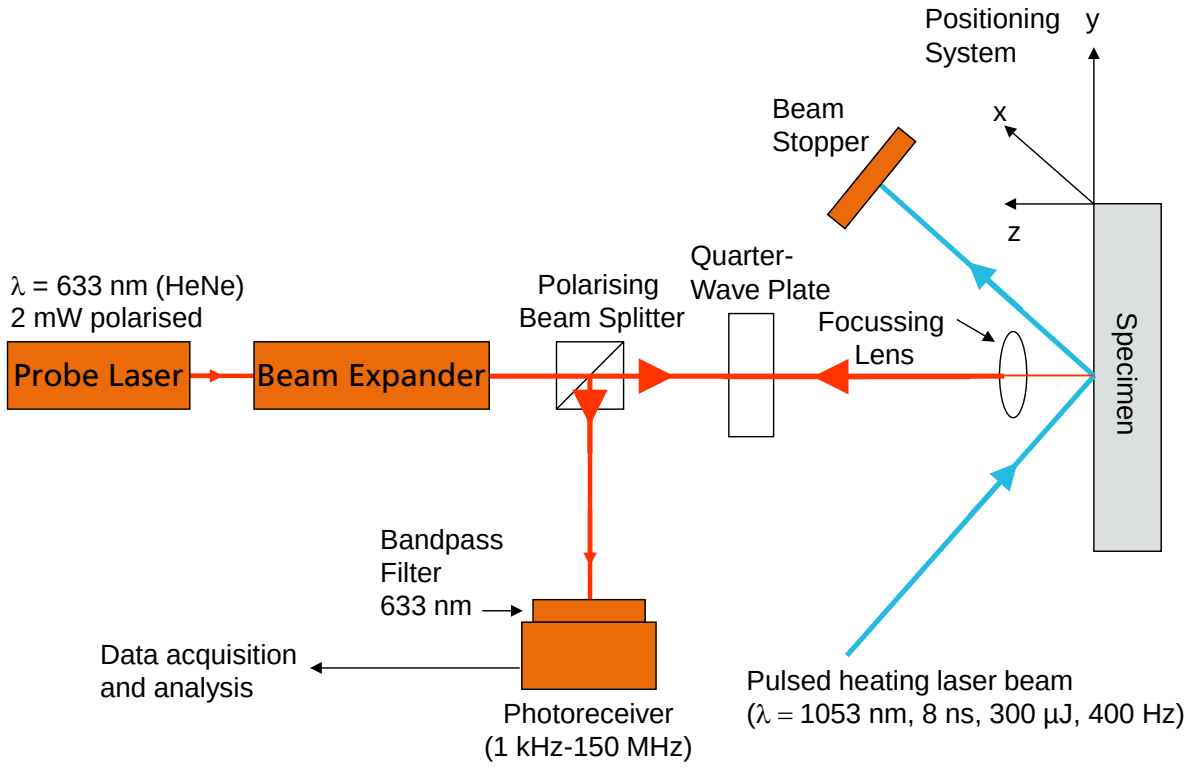

Fig. 1 Outline of the experimental Set-Up

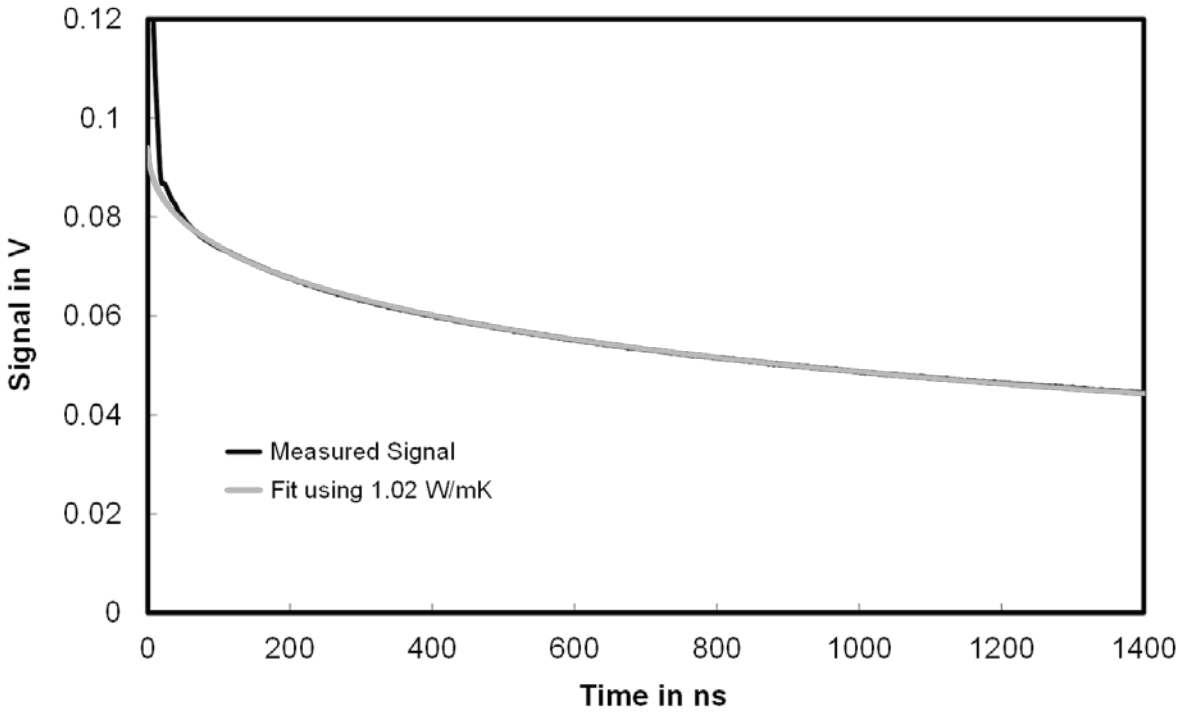

Fig.2: Measured signal (black) and signal fitted with Eq. (1) (grey) for soda-lime-glass coated with 810 nm Mo.

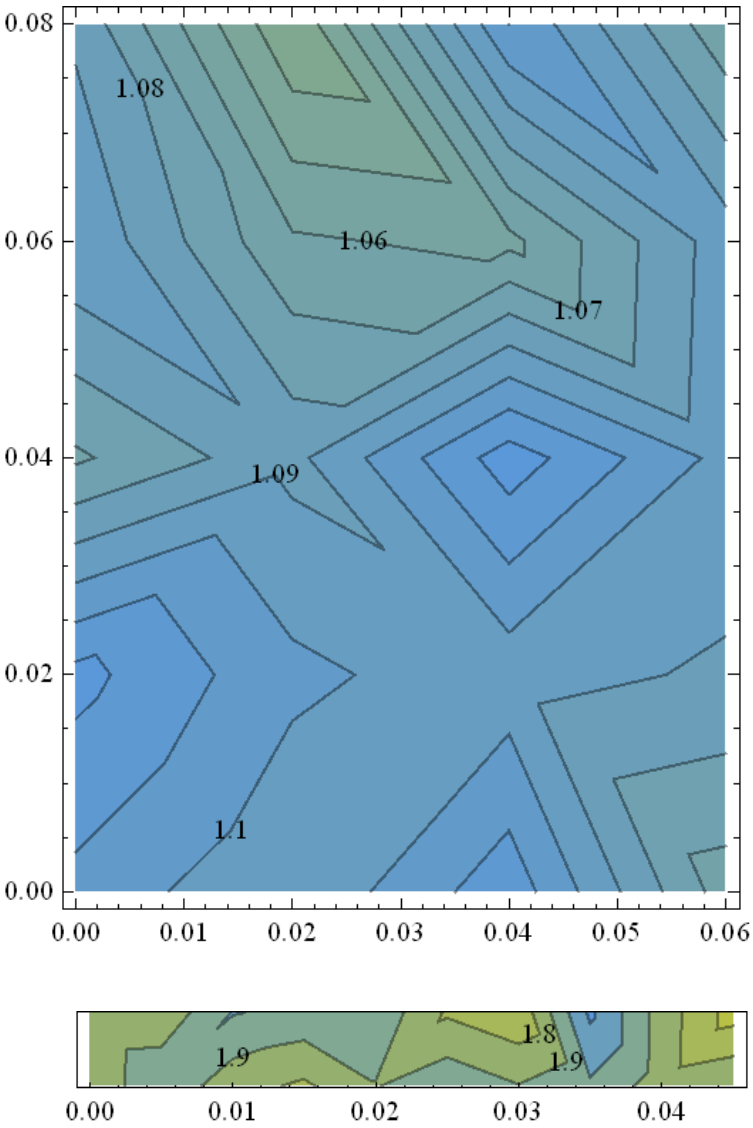

Fig.3 Above: Contour map of the thermal conductivity of a soda-lime glass surface. The numbers next to the contour lines correspond to the thermal conductivity in W/mK. Below: Contour map of the thermal conductivity of a PbTe surface. The numbers next to the contour lines correspond to the thermal conductivity in W/mK, the numbers on the x- and y-axis correspond to millimeters.

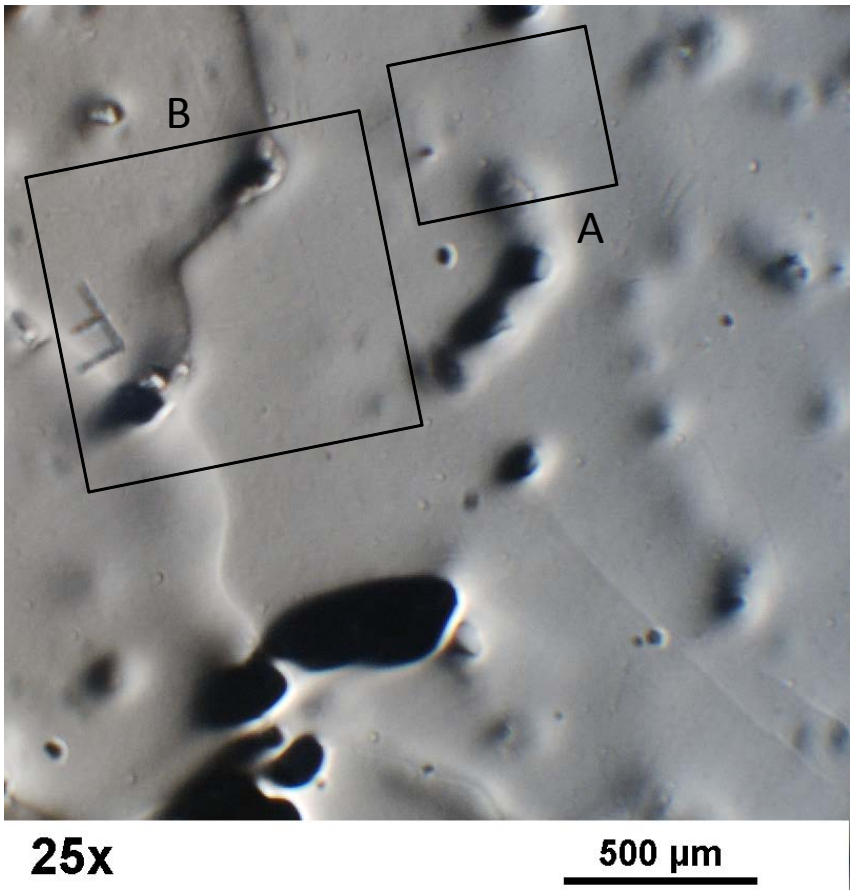

Fig. 4 Optical Micrograph of a LAST-18 specimen. The squares represent the scanned regions. The mark “F” was prepared by focused ion beam milling in order to unambiguously identify the scanned surface area.

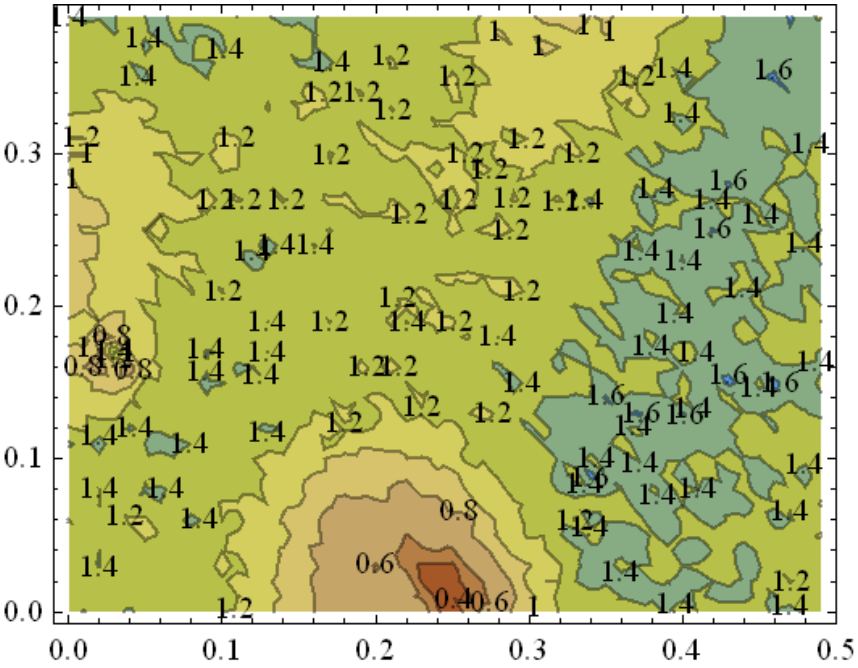

Fig. 5 Contour map of the thermal conductivity of a LAST-18 surface recorded from the region A marked in Fig. 4. The numbers next to the contour lines correspond to the thermal conductivity in W/mK. The map size is 500 x 400 µm.

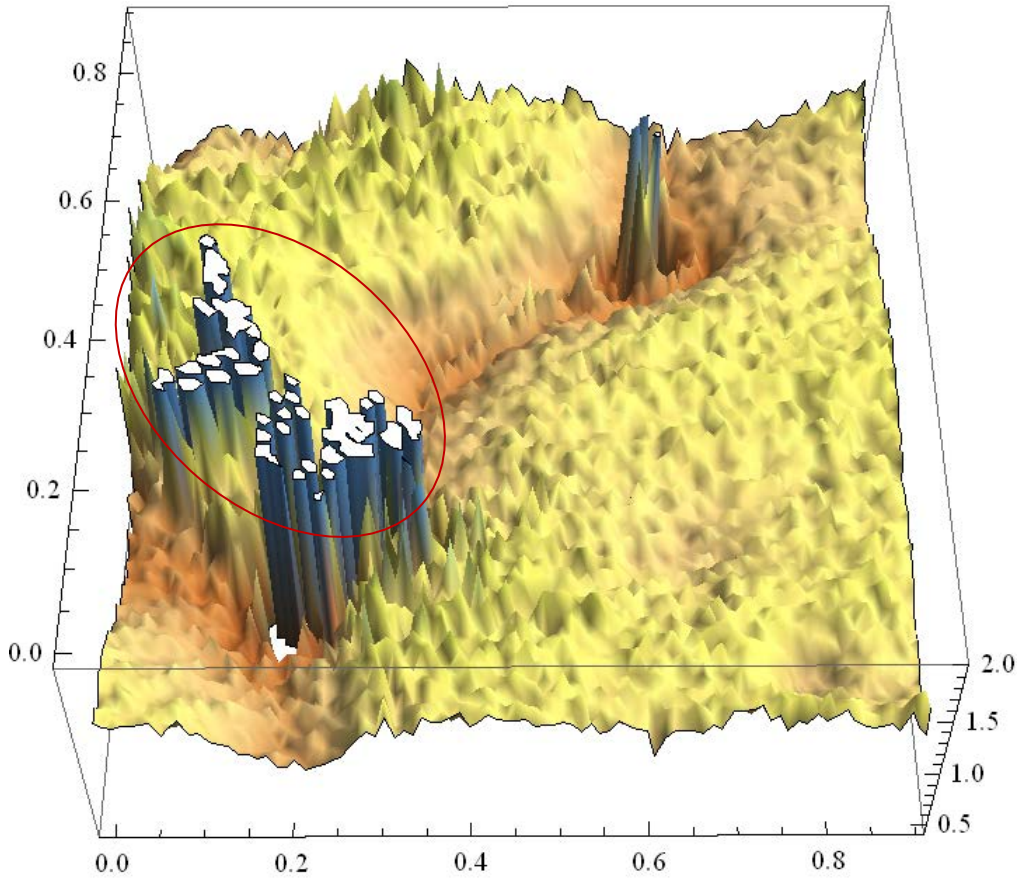

Fig. 6) Three-dimensional thermal conductivity map of region B in Fig. 4. The size of the map is 900 x 900 µm, the vertical scale corresponds to 0.4-2 W/mK.

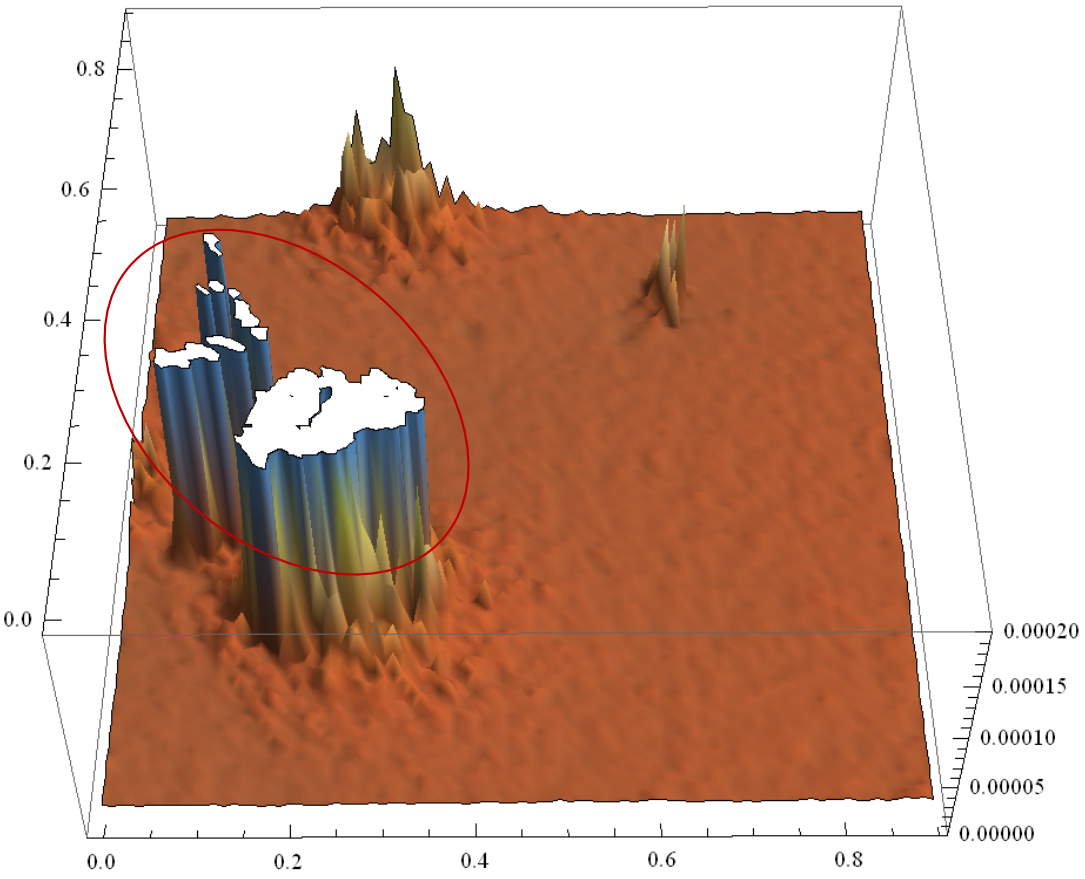

Fig. 7 Three-dimensional map of the RMS fitting error of the scan shown in Fig.6.

References

[1] A. Salazar; A. Sanchez-Lavega, A. Ocariz; J. Guitonny; G.C. Pandey; D. Fournier; A.C. Boccara, J. Appl. Phys. 79, 3984-93 (1996)

[2] M. Bertolotti, G. Liakhou, R. Li Voti, F. Michelotti, C. Sibilia, J. Appl. Phys. 74, 7078-7084 (1993)

[3] A.J. Schmidt, R. Cheaito, M. Chiesa, J. Appl. Phys. 107, 024908 (2010)

[4] S. Huxtable, D.G. Cahill, V. Fauconnier, J.O. White, J.-C. Zhao, Nature Materials 3, 298-301 (2004)

[5] X. Zheng, D.G. Cahill, J.-C. Zhao, Adv.Eng.Materials 7, 622 (2005)

[6] B. Li, L. Pottier, J.P. Roger, D. Fournier, K. Watari, K. Hirato, J. Eur. Ceram. Soc. 19, 1631-39 (1999)

[7] N. Taketoshi, T. Baba, A. Ono in Thermal Conductivity 24 /Thermal Expansion 12, ed. By P.S. Gaal, D.E. Apostolescu, E.P. Hurst II (Technomic Publishing, Lancaster, Basel 1999), pp. 289-302

[8] S. Bai, Z. Tang, Z. Huang, J. Yu, IEEE Transactions on Industrial Electronics 56, 3238-43 (2009)

[9] O. W. Käding, H. Skurk, K. E. Goodson, Appl. Phys. Lett. 65, 1629-31 (1994)

[10] S. Andre, A. Degiovanni, Glastech.Ber. 66, 291-298 (1993)

[11] E. Bozorg-Grayeli, Z. Li, M. Asheghi, G. Delgado, M. Panzer, D. Wack, K. E. Goodson, J. Appl. Phys. 112, 083504 (2012)

[12] J. Dadda, E. Müller, S. Perlt, T. Höche, P. B. Pereira und R. P. Hermann, J Mater. Res. 26, 1800-12 (2011)